Direct Observation of the Relationship Between Molecular Topology and Bulk Morphology for a π-Conjugated Material

Martin T. Seifrid[†], G. N. Manjunatha Reddy[‡], Cheng Zhou[†], Bradley F. Chmelka[‡]*, Guillermo C. Bazan[†]*

[†]Center for Polymers and Organic Solids, Department of Chemistry and Biochemistry, University of California, Santa Barbara, California, 93106, United States

[‡]Department of Chemical Engineering, University of California, Santa Barbara, California, 93106, United States

Electronic Supplementary Information

Materials and methods

UV-visible absorption spectroscopy: UV-vis absorption spectra were recorded on a Perkin Elmer Lambda 750 UV-Vis spectrometer. The solution spectrum was determined by dissolving TT in chloroform at 0.01 mg/mL. Thin film absorbance measurements were performed using glass as the substrate, and the material was spin coated for 60 s at 1500 rpm at 10 mg/mL in chloroform. Absorbance measurements of the ordered solid and amorphous state were performed at ~ 115 ºC and after quickly cooling to room temperature from ~ 135 ºC. Thin film heating was accomplished by using a heated sample mount. The temperature was measured with an external thermocouple probe.

Solution-state NMR spectroscopy*:* Solution-state ^{1}H and ^{13}C NMR were used to characterize TT. Approximately 10 mg of TT dissolved in 1,1,2,2-tetrachloroethane-d_2 and transferred into a 4 mm NMR tube. All NMR experiments were carried out at room temperature on a Bruker 18.8 T AVANCE-II NMR spectrometer (^{1}H and ^{13}C Larmor frequencies were 800.24 MHz and 200 MHz, respectively) equipped with 4 mm B-B-O probe. The ^{1}H and ^{13}C 90° pulse lengths were of 11 μs and 9 μs, respectively. One-dimensional (1D) ^{1}H NMR spectrum was acquired by co-adding 8 transients using a relaxation delay of 2 s. 1D ^{13}C NMR spectrum was acquired by co-adding1024 transients using a relaxation delay of 2 s corresponding to an experimental time of 1h. WALTZ-16 heteronuclear decoupling[1] was used during the acquisition of ^{13}C spectrum with ^{1}H 180° pulse duration of 60 μs. To identify and distinguish *J*-mediated through-bond ^{1}H-^{1}H and ^{1}H-^{13}C moieties, two-dimensional (2D) ^{1}H{^{1}H} correlation (COSY) and 2D ^{1}H{^{13}C} heteronuclear multiple-bond correlation (HMBC) NMR spectra were acquired and analyzed. 2D ^{1}H{^{1}H} spectrum was acquired using 128 t_1 increments using an incremental time of 114 μs, each by co-adding 2 transients, with a recycle delay of 2 s corresponding to an experimental time of 16 mins. 2D ^{1}H{^{13}C} HMBC spectra were acquired using 3.4 ms ($1/2J_{CH}$, where, J_{CH} = 145 Hz) and 250 ms (i.e., $1/2J_{CH}$, where, J_{CH} = 2 Hz) mixing times, each using 76 t_1 increments with an incremental time of 14.6 μs and by the co-addition of 96 transients with a recycle delay of 2 s corresponding to a total experimental time of 7 h. All ^{1}H and ^{13}C experimental shifts are calibrated with respect to ^{1}H and ^{13}C signals of 1,1,2,2-tetrachloroethane-d_2 at 6.0 and 73.8 ppm, respectively.

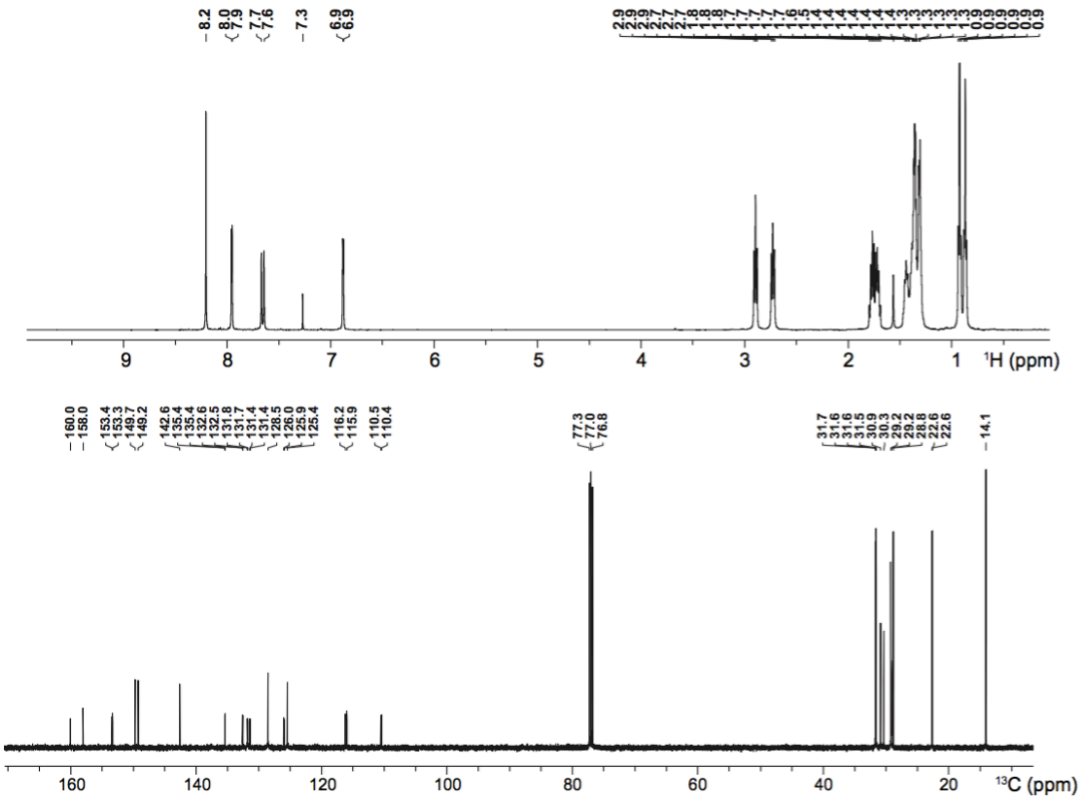

Figure S1. Solution-state ^{1}H and ^{13}C NMR spectra of TT dissolved in 1,1,2,2-tetrachloroethane-d_2 acquired at 18.8 T (^{1}H 800 MHz) at room temperature.

Solution-state ^{1}H and ^{13}C chemical shifts and splittings for the backbone moieties of TT are listed below.

^{1}H solution-state NMR in 1,1,2,2-tetrachloroethane-d_2 (ppm):
8.26 (s, 2H), 8.05 (d, J=3.2 Hz, 2H), 7.77 (d, J=12.9 Hz, 2H), 6.97 (d, J=2.9 Hz, 2H)
^{13}C solution-state NMR in 1,1,2,2-tetrachloroethane-d_2, δ (ppm):
159.2, 153.5, 149.9, 149.7, 142.9, 135.4, 132.7, 132.0, 131.5, 129.0, 126.2, 125.8, 116.3, 110.5

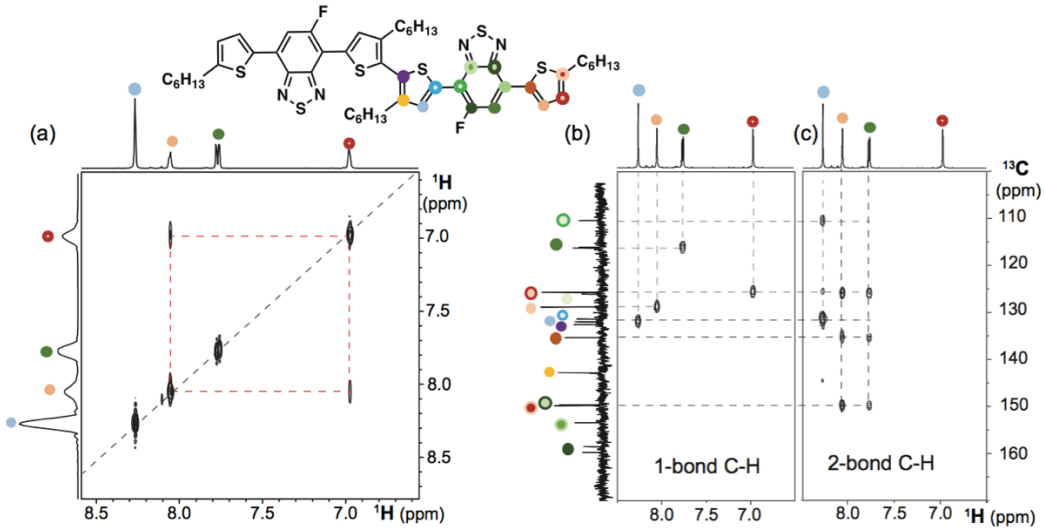

Figure S2. Solution-state 2D $^{1}H\{^{1}H\}$ correlation (COSY) spectrum of TT dissolved in 1,1,2,2-tetrachloroethane-d_2 acquired at 18.8 T (^{1}H 800 MHz) at room temperature. Off diagonal correlation intensities shown in dashed red lines depict the through-bond interactions between thiophene protons.

***Solid-state MAS NMR spectroscopy**:* A powder of TT was packed into a 4 mm (outer diameter) zirconia rotor fitted with Teflon insert and a ceramic cap fitted with a rubber *o*-ring to ensure close fitting of the sample. All variable temperature 1D and 2D MAS NMR spectra of TT were acquired on a 11.7 T Bruker AVANCE-II NMR spectrometer equipped with 4 mm H-X-Y probehead and Bruker VT control unit to regulate probe temperature. The ^{1}H and ^{13}C 90º pulse durations were 2.5 µs and 4.0 µs, respectively. To ensure the melt state of TT, single-pulse ^{13}C NMR spectrum was acquired at 135 ºC under a static condition by co-adding 2048 transients using a relaxation delay of 2 s corresponding to an experimental time of 2 h. For TT in the solid state, 1D $^{13}C\{^{1}H\}$ CP-MAS spectra were acquired at 118 ºC using 0.1 ms and 2 ms of CP contact times under 8 kHz MAS conditions using a stream of N_2 gas. Cross polarization involves the simultaneous excitation of ^{1}H and ^{13}C nuclei to enhance the signals of the latter. Heteronuclear decoupling was applied during acquisition of ^{13}C spectra using SPINAL64 sequence[2] using 2048 co-added transients with a 3 s recycle delay, corresponding to an experimental time of 2 h each. To characterize spatially proximate dipole-dipole coupled ^{1}H-^{13}C pairs, 2D $^{13}C\{^{1}H\}$ heteronuclear correlation (HETCOR) NMR spectra were acquired using a short (0.1 ms) and long (2 ms) CP contact times. 2D $^{13}C\{^{1}H\}$ HETCOR NMR spectra were acquired using 32 t_1 increments using an incremental time of 80 µs, each by co-adding 256 transients with a relaxation delay of 3 s corresponding to an experimental time of 7 h each.

All ^{1}H and ^{13}C experimental shifts are calibrated with respect to neat TMS using adamantane as an external reference (higher ppm ^{13}C resonance, 35.8 ppm[3] and the ^{1}H resonance, 1.85 ppm[4]).

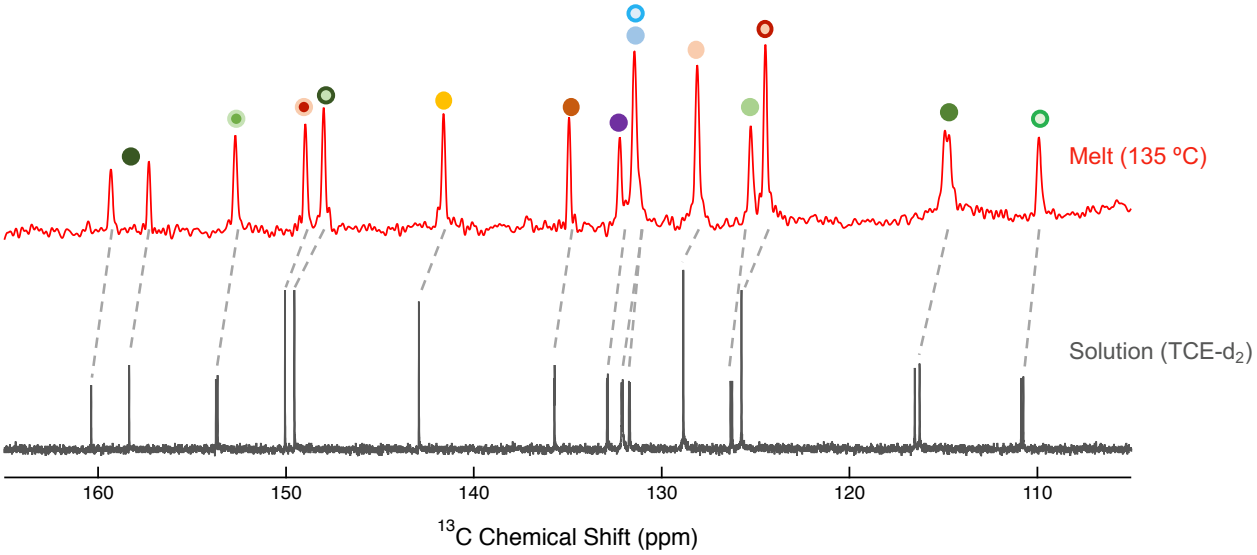

Figure S3. Comparison of single-pulse ^{13}C NMR spectrum of TT acquired at 135 ºC (melt) and the analogous ^{13}C NMR spectrum of TT dissolved in 1,1,2,2-tetrachloroethane-d_2 acquired at room temperature.

Aromatic ^{13}C chemical shifts of TT measured at 135 ºC (melt) and at 118 ºC (ordered solid) are given below.

^{13}C NMR in the melt (135 ºC), δ (ppm):
159.4, 157.4, 152.8, 149.1, 148.1, 141.7, 135.0, 132.3, 131.5, 131.5, 128.2, 125.3, 124.6, 114.9, 110.0
^{13}C solid-state NMR of the solid (118 ºC), δ (ppm):
159.2, 157.6, 154.2, 150.9, 147.6, 139.8, 139.8, 134.3, 132.6, 132.6, 129.7, 123.8, 123.8, 115.4, 110.4

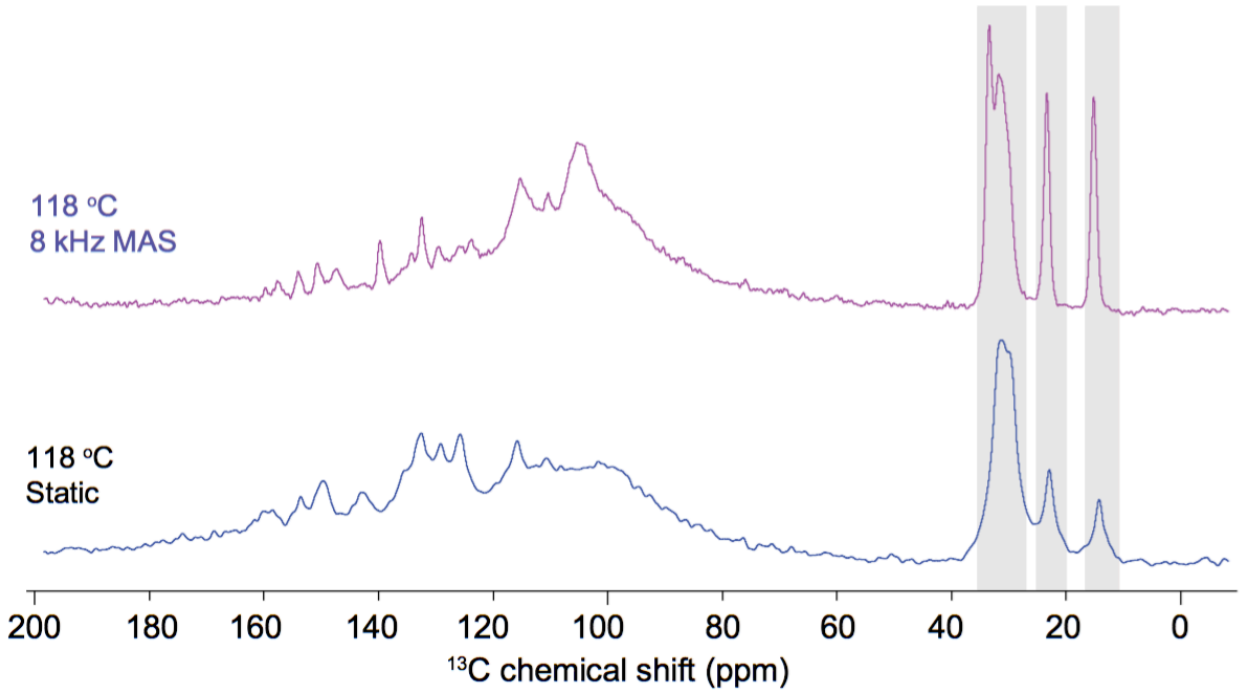

Figure S4. Solid-state single-pulse ^{13}C NMR spectra of TT acquired at 11.7 T and 118 ºC using MAS (top) and static (bottom) conditions. Shaded regions highlight similarities in signal intensities and line widths and suggest the presence of disordered alkyl side chains, whereas the broad spectral features observed in the aromatic region (110 – 160 ppm) of the spectrum acquired under static conditions suggest well ordered, π-π stacked TT backbones.

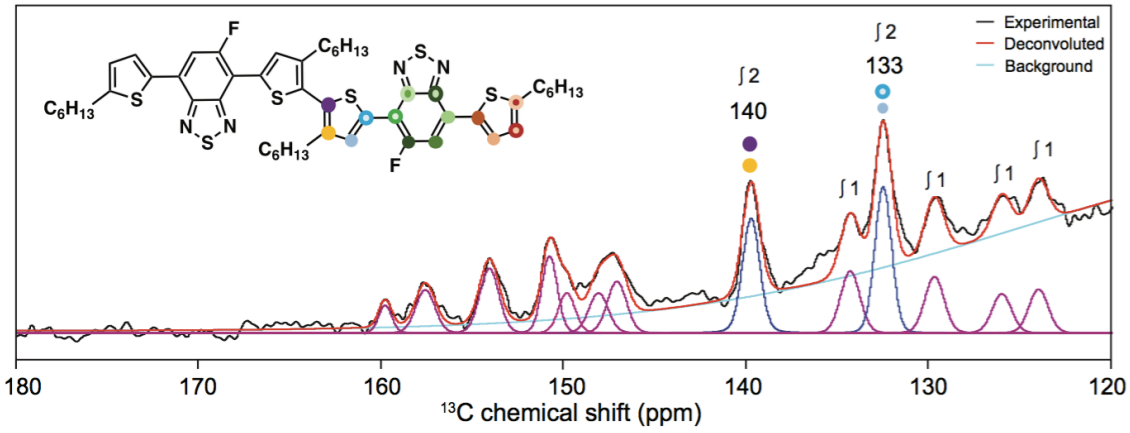

Figure S5. Solid-state single-pulse ^{13}C NMR spectrum of TT acquired at 11.7 T and 118 ºC using high-power ^{1}H-decoupling. Integrals measured from the deconvolution of the spectrum reveal that the signals at 140 and 133 ppm are the overlapping contributions from two different carbon signals.

For TT in the lamellar state at 118 ºC, the local structures of the central and peripheral thiophene groups are elucidated by analyzing 2D $^{13}C\{^{1}H\}$ HETCOR NMR spectra (Figure S6); in the spectrum acquired using 0.1 ms CP contact time, correlated signal intensities at 134 ppm (^{13}C) and 7.6 ppm (^{1}H) correspond to directly bonded ^{13}C-^{1}H of central thiophene (blue dot), and at 130 ppm (^{13}C) and 7.4 ppm (^{1}H) and 115 ppm (^{13}C) and 6.9 ppm (^{1}H) indicate the directly bonded ^{13}C-^{1}H in fluorobenzothiadiazole and thiophene end groups, respectively. In the 2D $^{13}C\{^{1}H\}$ HETCOR NMR

spectrum acquired using 2 ms of CP contact time, correlation intensities originate from thiophene ^{13}C and alkyl sidechain ^{1}H moieties are observed as depicted by dashed horizontal and vertical lines in Figure S6b.

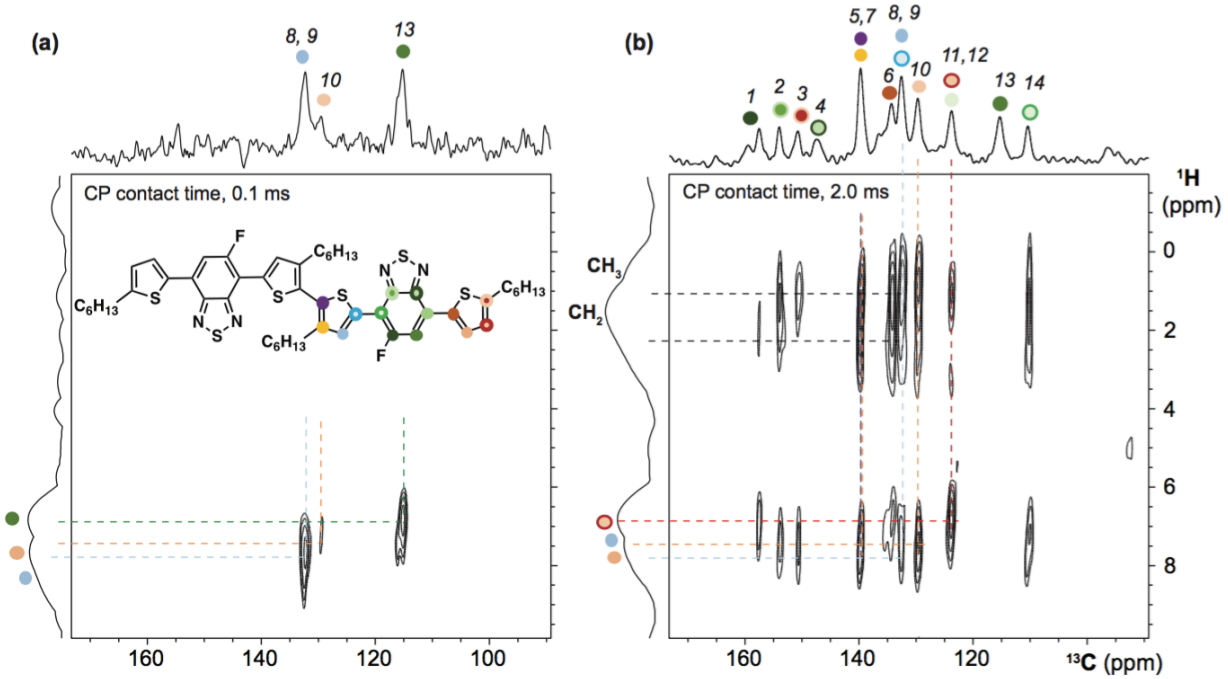

Figure S6. Solid-state 2D $^{13}C\{^{1}H\}$ HETCOR NMR spectrum recorded at 11.7 T and at 118 ºC using (a) 0.1 ms and (b) 2 ms of CP contact times, respectively.

DFT calculations: All calculations were performed using the Gaussian 09 software package.[5] The B3LYP functional and 6-31G(d,p) basis set were used to optimize the ground-state equilibrium geometry of TT. For the planar conformation, the central S-C-C-S dihedral was frozen at 180º and the rest of the structure was allowed to optimize the ground-state equilibrium geometry. The twisted conformation of TT was allowed to relax to the lowest energy conformation without any constraints. For each conformer of TT, the range-separation parameter ω in the ωB97XD functional was tuned using the gap tuning procedure.[6] The structures were subsequently optimized to their ground-state equilibrium geometries using the tuned ωB97XD/6-31G(d,p) functional and basis set by the same methods described above; ω = 0.1253 $bohr^{-1}$ for the twisted conformer and ω = 0.1081 $bohr^{-1}$ for the trans-planar conformer. These optimized geometries were used to calculate magnetic shieldings using the gauge-independent atomic orbital (GIAO) method in a conductor-like polarizable continuum model (CPCM)[7] for a conjugated organic material (where the static dielectric constant is set to ε = 3.5 and the dynamic dielectric constant is set to $\varepsilon_{inf} = 2$)[8] with the tuned ωB97XD functional and 6-311+G(2d,p) basis set. Plots of experimental ^{13}C chemical shifts versus GIAO DFT-calculated NMR chemical shifts are shown in Figure S7 for the planar and twisted TT conformations.

Based on calculations of different possible rota-mers for both the twisted and planar confor-mations of TT, planarization of the molecule may also involve a flip of the fluorobenzothiadiazole (FBT) heterocycles and outer thiophene rings. This additional reconfiguration is reasonable, as single crystal data for similar compounds have shown a multitude of rotamer populations.[9–11]

Computationally predicted chemical shieldings, σ_{iso}, can be compared to experimental isotropic chemical shifts, δ_{iso}, by using the following conversion,[12–17]

$$\delta_{iso} = \frac{intercept - \sigma_{iso}}{-slope} \quad (1)$$

where *intercept* and *slope* are the intercept and slope determined from linear regression analysis in Figure S7.

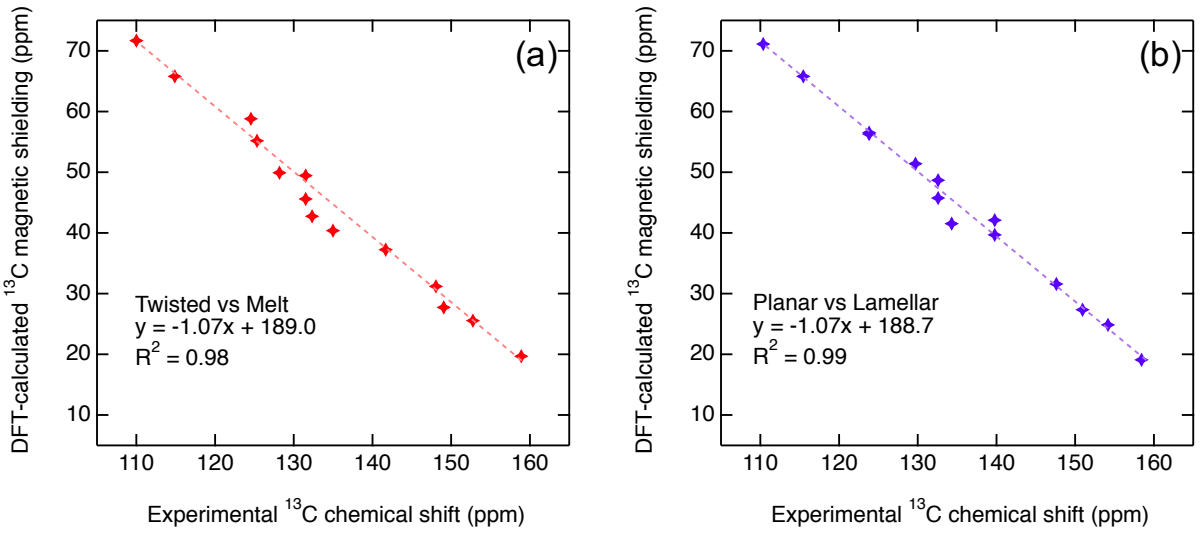

Figure S7. Plots of DFT-calculated ^{13}C chemical shieldings versus experimental ^{13}C chemical shifts obtained for the twisted (a) and planar (b) conformations of TT models from the high-temperature ^{13}C NMR spectra acquired at 135 ºC and 118 ºC, respectively. Regression analyses are presented in figure insets, which depict reasonably good agreements with R^2 values 0.98 and 0.99 for the twisted and planar conformers of TT, respectively.

DFT-calculated isotropic ^{13}C chemical shieldings for the backbone carbon atoms of TT are given below.

Twisted conformer, σ_{iso} (ppm):
19.6941, 25.5663, 27.7351, 31.2094, 37.257, 40.3939, 42.7596, 45.6088, 49.4673, 49.9177, 55.1814, 58.8164, 65.7932, 71.682
Planar conformer, σ_{iso} (ppm):
19.1113, 24.8516, 27.3565, 31.6064, 39.6791, 41.5304, 42.1121, 45.7494, 48.6781, 51.4214, 56.2908, 56.5454, 65.8058, 71.1200

References

(1) Shaka, A. J.; Keeler, J.; Frenkiel, T.; Freeman, R. An Improved Sequence for Broadband Decoupling: WALTZ-16. *J. Magn. Reson. 1969* **1983**, *52* (2), 335–338.

(2) Khitrin, A.; Fung, B. M. Design of Heteronuclear Decoupling Sequences for Solids. *J. Chem. Phys.* **2000**, *112* (5), 2392–2398.

(3) Morcombe, C. R.; Zilm, K. W. Chemical Shift Referencing in MAS Solid State NMR. *J. Magn. Reson.* **2003**, *162* (2), 479–486.

(4) Hayashi, S.; Hayamizu, K. Chemical-Shift Standards in High-Resolution Solid-State Nmr (1) 13C, 29Si and 1H Nuclei. *Bull. Chem. Soc. Jpn.* The Chemical Society of Japan 公益社団法人 日本化学会 February 7, 1991, pp 685–687.

(5) Frisch, M. J.; Trucks, G. W.; Schlegel, H. B.; Scuseria, G. E.; Robb, M. A.; Cheeseman, J. R.; Scalmani, G.; Barone, V.; Mennucci, B.; Petersson, G. A.; Nakatsuji, H.; Caricato, M.; Li, X.; Hratchian, H. P.; Izmaylov, A. F.; Bloino, J.; Zheng, G.; Sonnenberg, J. L.; Hada, M.; Ehara, M.; Toyota, K.; Fukuda, R.; Hasegawa, J.;

Ishida, M.; Nakajima, T.; Honda, Y.; Kitao, O.; Nakai, H.; Vreven, T.; Montgomery, J. A.; Peralta, J. E.; Ogliaro, F.; Bearpark, M.; Heyd, J. J.; Brothers, E.; Kudin, K. N.; Staroverov, V. N.; Keith, T.; Kobayashi, R.; Normand, J.; Raghavachari, K.; Rendell, A.; Burant, J. C.; Iyengar, S. S.; Tomasi, J.; Cossi, M.; Rega, N.; Millam, J. M.; Klene, M.; Knox, J. E.; Cross, J. B.; Bakken, V.; Adamo, C.; Jaramillo, J.; Gomperts, R.; Stratmann, R. E.; Yazyev, O.; Austin, A. J.; Cammi, R.; Pomelli, C.; Ochterski, J. W.; Martin, R. L.; Morokuma, K.; Zakrzewski, V. G.; Voth, G. A.; Salvador, P.; Dannenberg, J. J.; Dapprich, S.; Daniels, A. D.; Farkas, O.; Foresman, J. B.; Ortiz, J. V.; Cioslowski, J.; Fox, D. J. Gaussian 09, Revision D.01. Gaussian, Inc.: Wallingford, CT 2016.

(6) Sun, H.; Zhong, C.; Brédas, J.-L. Reliable Prediction with Tuned Range-Separated Functionals of the Singlet–Triplet Gap in Organic Emitters for Thermally Activated Delayed Fluorescence. *J. Chem. Theory Comput.* **2015**, *11* (8), 3851–3858.

(7) Takano, Y.; Houk, K. N. Benchmarking the Conductor-like Polarizable Continuum Model (CPCM) for Aqueous Solvation Free Energies of Neutral and Ionic Organic Molecules. *J. Chem. Theory Comput.* **2005**, *1* (1), 70–77.

(8) Sun, H.; Ryno, S.; Zhong, C.; Ravva, M. K.; Sun, Z.; Körzdörfer, T.; Brédas, J.-L. Ionization Energies, Electron Affinities, and Polarization Energies of Organic Molecular Crystals: Quantitative Estimations from a Polarizable Continuum Model (PCM)-Tuned Range-Separated Density Functional Approach. *J. Chem. Theory Comput.* **2016**, *12* (6), 2906–2916.

(9) Van Der Poll, T. S.; Zhugayevych, A.; Chertkov, E.; Bakus, R. C.; Coughlin, J. E.; Teat, S. J.; Bazan, G. C.; Tretiak, S. Polymorphism of Crystalline Molecular Donors for Solution-Processed Organic Photovoltaics. *J. Phys. Chem. Lett.* **2014**, *5* (15), 2700–2704.

(10) Coughlin, J. E.; Zhugayevych, A.; Bakus, R. C.; van der Poll, T. S.; Welch, G. C.; Teat, S. J.; Bazan, G. C.; Tretiak, S. A Combined Experimental and Theoretical Study of Conformational Preferences of Molecular Semiconductors. *J. Phys. Chem. C* **2014**, *118* (29), 140627161810001.

(11) McDowell, C.; Narayanaswamy, K.; Yadagiri, B.; Gayathri, T.; Seifrid, M.; Datt, R.; Ryno, S. M.; Heifner, M. C.; Gupta, V.; Risko, C.; Singh, S. P.; Bazan, G. C. Impact of Rotamer Diversity on the Self-Assembly of Nearly Isostructural Molecular Semiconductors. *J. Mater. Chem. A* **2018**, *6* (2), 383–394.

(12) Lodewyk, M. W.; Siebert, M. R.; Tantillo, D. J. Computational Prediction of ^{1}H and ^{13}C Chemical Shifts: A Useful Tool for Natural Product, Mechanistic, and Synthetic Organic Chemistry. *Chem. Rev.* **2012**, *112* (3), 1839–1862.

(13) Pierens, G. K. ^{1}H and ^{13}C NMR Scaling Factors for the Calculation of Chemical Shifts in Commonly Used Solvents Using Density Functional Theory. *J. Comput. Chem.* **2014**, *35* (18), 1388–1394.

(14) Benassi, E. Benchmarking of Density Functionals for a Soft but Accurate Prediction and Assignment of ^{1}H and ^{13}C NMR Chemical Shifts in Organic and Biological Molecules. *J. Comput. Chem.* **2017**, *38* (2), 87–92.

(15) Konstantinov, I. A.; Broadbelt, L. J. Regression Formulas for Density Functional Theory Calculated ^{1}H and ^{13}C NMR Chemical Shifts in Toluene-d_8. *J. Phys. Chem. A* **2011**, *115* (44), 12364–12372.

(16) Reddy, G. N. N. M.; Cook, D. S.; Iuga, D.; Walton, R. I.; Marsh, A.; Brown, S. P. An NMR Crystallography Study of the Hemihydrate of 2′, 3′-O-Isopropylidineguanosine. *Solid State Nucl. Magn. Reson.* **2015**, *65*, 41–48.

(17) Reddy, G. N. M.; Marsh, A.; Davis, J. T.; Masiero, S.; Brown, S. P. Interplay of Noncovalent Interactions in Ribbon-like Guanosine Self-Assembly: An NMR Crystallography Study. *Cryst. Growth Des.* **2015**, *15* (12), 5945–5954.